

DESY 09-044, FTUV-09-0112, ICCUB-09-193,  
 IFIC/09-02, LPT-Orsay/09-18, ROM2F/2009/05,  
 RM3-TH/09-7, SFB/PPP-09-32, UB-ECM-PF 09/08

# Pseudoscalar decay constants of kaon and $D$ -mesons from $N_f = 2$ twisted mass Lattice QCD



**B. Blossier<sup>(a,b)</sup>, P. Dimopoulos<sup>(c)</sup>, R. Frezzotti<sup>(c)</sup>, B. Haas<sup>(b)</sup>,  
 G. Herdoiza<sup>(a)</sup>, K. Jansen<sup>(a)</sup>, V. Lubicz<sup>(d,e)</sup>, F. Mescia<sup>(f)</sup>, D. Palao<sup>(g)</sup>,  
 A. Shindler<sup>(h)</sup>, S. Simula<sup>(e)</sup>, C. Tarantino<sup>(d,e)</sup>, C. Urbach<sup>(i)</sup>**

<sup>(a)</sup> DESY, Zeuthen, Platanenallee 6, D-15738 Zeuthen, Germany

<sup>(b)</sup> Laboratoire de Physique Théorique (Bât. 210), Université de Paris XI,  
 Centre d'Orsay, 91405 Orsay-Cedex, France

<sup>(c)</sup> Dip. di Fisica, Università di Roma Tor Vergata and INFN, Sez. di Roma Tor Vergata,  
 Via della Ricerca Scientifica, I-00133 Roma, Italy

<sup>(d)</sup> Dip. di Fisica, Università di Roma Tre, Via della Vasca Navale 84, I-00146 Roma, Italy

<sup>(e)</sup> INFN, Sez. di Roma III, Via della Vasca Navale 84, I-00146 Roma, Italy

<sup>(f)</sup> Departament d'Estructura i Constituents de la Matèria and Institut de Ciències del Cosmos  
 (ICCUB), Universitat de Barcelona, Diagonal 647, 08028 Barcelona, Spain

<sup>(g)</sup> Dep. de Física Teòrica and IFIC, Univ. de València, Dr. Moliner 50, E-46100 Burjassot, Spain

<sup>(h)</sup> Theoretical Physics Division, Dept. of Mathematical Sciences,  
 University of Liverpool, Liverpool L69 7ZL, UK

<sup>(i)</sup> Institut für Elementarteilchenphysik, Fachbereich Physik,  
 Humbolt Universität zu Berlin, D-12489, Berlin, Germany

## Abstract

We present the results of a lattice QCD calculation of the pseudoscalar meson decay constants  $f_\pi$ ,  $f_K$ ,  $f_D$  and  $f_{D_s}$ , performed with  $N_f = 2$  dynamical fermions. The simulation is carried out with the tree-level improved Symanzik gauge action and with the twisted mass fermionic action at maximal twist. We have considered for the final analysis three values of the lattice spacing,  $a \simeq 0.10$  fm, 0.09 fm and 0.07 fm, with pion masses down to  $m_\pi \simeq 270$  MeV. Our results for the light meson decay constants are  $f_K = 158.1(2.4)$  MeV and  $f_K/f_\pi = 1.210(18)$ . From the latter ratio, by using the experimental determination of  $\Gamma(K \rightarrow \mu\bar{\nu}_\mu(\gamma))/\Gamma(\pi \rightarrow \mu\bar{\nu}_\mu(\gamma))$  and the average value of  $|V_{ud}|$  from nuclear beta decays, we obtain  $|V_{us}| = 0.2222(34)$ , in good agreement with the determination from semileptonic  $K_{l3}$  decays and the unitarity constraint. For the  $D$  and  $D_s$  meson decay constants we obtain  $f_D = 197(9)$  MeV,  $f_{D_s} = 244(8)$  MeV and  $f_{D_s}/f_D = 1.24(3)$ . Our result for  $f_D$  is in good agreement with the CLEO experimental measurement. For  $f_{D_s}$  our determination is smaller than the PDG 2008 experimental average but in agreement with a recent improved measurement by CLEO at the  $1.4\sigma$  level.

## 1 Introduction

An accurate lattice determination of the pseudoscalar decay constants of kaon and  $D$ -mesons is an important task. On the one hand, the ratio  $f_K/f_\pi$  can be used together with the experimental determination of  $\Gamma(K \rightarrow \mu\bar{\nu}_\mu(\gamma))/\Gamma(\pi \rightarrow \mu\bar{\nu}_\mu(\gamma))$  and the average value of  $|V_{ud}|$  from nuclear beta decays to achieve a precise determination of the CKM matrix element  $|V_{us}|$  [1] and to test the CKM first row unitarity relation. On the other hand, the pseudoscalar decay constants  $f_D$  and  $f_{D_s}$  have been recently measured at CLEO, BaBar and Belle [2, 3], asking for accurate lattice determinations to be compared to.

In this paper, we present a lattice QCD calculation of the pseudoscalar meson decay constants  $f_\pi$ ,  $f_K$ ,  $f_D$  and  $f_{D_s}$ . With respect to our previous study of the pion and kaon decay constants [4], here we have analysed data at three values of the lattice spacing,  $a \simeq 0.10$  fm, 0.09 fm, 0.07 fm (corresponding to  $\beta = 3.8, 3.9, 4.05$ ), and performed a chiral extrapolation taking lattice artefacts into account. Estimating the lattice artefacts turns out to be crucial for an accurate determination of  $f_D$  and  $f_{D_s}$  since cutoff effects induced by the charm mass, which are parametrically of  $\mathcal{O}(a^2 m_c^2)$ , are not small in our simulation,  $\sim 5 \div 10\%$ . Both SU(2) and SU(3) chiral perturbation theory (ChPT) has been considered for the chiral extrapolation, whereas only the latter was considered in [4]. With respect to ref. [4], we have also added ensembles with a lighter quark mass ( $m_\pi \simeq 270$  MeV) and a larger volume ( $L \simeq 2.7$  fm), both at the value of  $a \simeq 0.09$  fm.

The calculation is based on the gauge field configurations generated by the European Twisted Mass Collaboration (ETMC) with the tree-level improved Symanzik gauge action [5] and the twisted mass action [6] at maximal twist, discussed in detail in refs. [7]-[10]. We simulated  $N_f = 2$  dynamical quarks, taken to be degenerate in mass, whose masses are eventually extrapolated to the physical isospin averaged mass of the up and down quarks. The strange and charm quarks are quenched in the present calculation.

The use of the twisted mass fermions turns out to be beneficial, since the pseudoscalar meson masses and decay constants, which represent the basic ingredients of the calculation,

are automatically improved at  $\mathcal{O}(a)$  [11] (see also [12]), and the determination of the pseudoscalar decay constants does not require the introduction of any renormalization constant. Both these features allow to significantly improve the accuracy of the calculation. It has also been shown that, for twisted mass fermions at maximal twist, the so called KLM factor [13], which relates the lattice quark propagator at zero momentum to the continuum one, is equal to one at tree level, to all order in  $am_q$  [14]. This is beneficial in reducing discretization effects particularly for heavy quark masses, as the charm quark mass considered in this study.

As discussed in refs. [4, 15, 16], we implement non-degenerate valence quarks in the twisted mass formulation by formally introducing a twisted doublet for each non-degenerate quark flavour. In the present analysis we thus introduce in the valence sector three twisted doublets,  $(u, d)$ ,  $(s, s')$  and  $(c, c')$ , with masses  $\mu_l$ ,  $\mu_s$  and  $\mu_c$  respectively. Within each doublet, the two valence quarks are regularized in the physical basis with Wilson parameters of opposite values ( $r = -r' = 1$ ). We simulate mesons composed of quarks with opposite Wilson parameters so that the squared meson mass  $m_{PS}^2$  differs from its continuum counterpart only by terms of  $\mathcal{O}(a^2 \mu_q)$  and  $\mathcal{O}(a^4)$ , whereas  $f_{PS}$  differs from its continuum limit by terms of  $\mathcal{O}(a^2)$  [17, 18]. This implies that at  $\mathcal{O}(a^2)$  the cutoff effects on  $m_{PS}^2$  and  $f_{PS}$  are as in a chiral invariant lattice formulation. In our calculation large artefacts, like those affecting the neutral pion mass in the twisted mass formulation of lattice QCD, seem not to be present.

In the present analysis, we study the pseudoscalar decay constants as a function of the meson masses, whereas in our previous work [4] we relied on their dependence on the quark masses. When data at different values of the lattice spacing are involved, the study in terms of meson masses is simpler, since it does not require the introduction of the quark mass renormalization constant ( $Z_m = Z_P^{-1}$ ) to convert at each lattice spacing from the bare to the renormalized (cutoff independent) quark mass. The dependence of the decay constants on the meson masses is studied together with the dependence on the lattice spacing, through a combined fit where terms of  $\mathcal{O}(a^2)$ , coming from the Symanzik expansion of the lattice theory, are added to the functional forms predicted by ChPT. In this way, the continuum and chiral extrapolations of the lattice results are performed simultaneously. In alternative to this combined analysis, a different approach could be adopted. It consists of first extrapolating data at fixed meson mass values to the continuum, and then extrapolating the obtained continuum results to the physical point. With our simulation setup, however, this procedure turns out to be unsafe, since for some values of the meson masses we have data at only two values of the lattice spacing. Such a procedure could become feasible when data at a smaller value of the lattice spacing are available. Corresponding simulations with  $a \simeq 0.05$  fm are currently performed by ETMC.

In order to perform the extrapolation to the physical masses we have used ChPT for the light mesons and Heavy Meson ChPT (HMChPT) [19] for the  $D$  sector. For the kaon and  $D_s$  mesons we have considered both SU(2)- and SU(3)-ChPT. In the SU(2) case one treats the  $u/d$  quarks as light, while the strange quark is not required to satisfy chiral symmetry. The short interpolation to the physical strange quark, which is required in our analysis, is then performed linearly [20]. This is justified, since our simulated values of the strange quark mass are around the physical mass. For comparison, we have also considered

chiral extrapolations based on SU(3)-ChPT and SU(3)-HMChPT. We find that the SU(2) effective theory, which is less predictive than SU(3), provides however a better description of the lattice data for the decay constants up to the region of the strange quark mass.

Our final results for the kaon and  $D$ -mesons decay constants are given in the abstract and in eqs. (11) and (23). Our determination of  $f_K/f_\pi$  leads to a determination of  $|V_{us}|$  that is in good agreement with the value obtained from semileptonic kaon decays, though with a larger error, as well as with the first row unitarity constraint of the CKM matrix. Of relevant phenomenological interest is also our result for  $f_{D_s}$ , which is about  $2.3\sigma$  lower than the experimental average quoted by the PDG [2] but in agreement with other unquenched lattice determinations and with a recent improved measurement by CLEO [3] at the  $1.4\sigma$  level. The value indicated by the new CLEO measurement weakens the tension between experimental and lattice results for  $f_{D_s}$ , which suggested explanations in terms of new physics effects [21, 22].

The plan of this paper is as follows. In section 2 we provide the details of the lattice simulations used for the present study and discuss the determination of the pseudoscalar meson masses and decay constants. The combined chiral and continuum extrapolation fits of the light and  $D$ -mesons decay constants are discussed in sections 3 and 4, respectively. There, we also provide our final results for the decay constants, discussing in particular the evaluation of the systematic uncertainties and the comparison with other lattice determinations and with recent experimental measurements.

## 2 Simulation details

Details of the ensembles of gauge configurations used in the present analysis and the values of the simulated valence quark masses are collected in Tables 1 and 2, respectively.

Measurements are performed over independent gauge configurations that are separated by 20 trajectories in the case of the ensembles at  $\beta = 3.8$  and  $3.9$ , and by 40 trajectories in the case of the ensembles at  $\beta = 4.05$ . The trajectory length is equal to unity for the ensembles  $A_2$ ,  $A_3$  and  $B_7$  and to  $1/2$  for the ensembles  $B_1$ - $B_4$ ,  $B_6$  and  $C_1$ - $C_3$ . Among the available ETMC ensembles we have excluded from this study those corresponding to pion masses larger than 500 MeV (ensembles  $A_4$ ,  $B_5$  and  $C_4$  of ref. [9]).

Our strategy and the conditions to tune to maximal twist have been discussed in refs. [7]-[9]. Whereas at  $\beta = 3.9$  and  $\beta = 4.05$  these conditions are accurately fulfilled, at  $\beta = 3.8$  the situation is different. Due to large fluctuations and long autocorrelations for the PCAC mass appearing at the smallest value of the twisted mass parameter at  $\beta = 3.8$ , we cannot be confident that the maximal twist condition is realized with the same accuracy as at  $\beta = 3.9$  and  $\beta = 4.05$ . In the present study, in order to check for effects of such a possible mismatch, besides not considering the ensemble with the lightest quark mass at  $\beta = 3.8$  (ensemble  $A_1$  of ref. [9]), we have also performed an analysis with and without taking the whole set of data at  $\beta = 3.8$  into account. As we will demonstrate below, fully consistent results are obtained. This finding is also supported by the results of a theoretical analysis of the effects of being out of maximal twist, which shows that these systematic effects on the pseudoscalar decay constants analyzed here at  $\beta = 3.8$  are small compared to statistical

Ens.	$\beta$	$a$ [fm]	$V/a^4$	$a\mu_{sea}$	$m_\pi$ [MeV]	$m_\pi L$	$N_{cfg}$	$(\Delta t)_{\pi,K}$	$(\Delta t)_{D,D_s}$
$A_2$	3.8	0.10	$24^3 \times 48$	0.0080	410	5.0	240	[10, 23]	[14, 23]
$A_3$				0.0110	480	5.8	240		
$B_1$	3.9	0.085	$24^3 \times 48$	0.0040	315	3.3	480	[12, 23]	[16, 23]
$B_2$				0.0064	390	4.0	240		
$B_3$				0.0085	450	4.7	240		
$B_4$				0.0100	490	5.0	240		
$B_7$	3.9	0.085	$32^3 \times 64$	0.0030	270	3.7	240	[12, 31]	[16, 31]
$B_6$				0.0040	310	4.3	240		
$C_1$	4.05	0.065	$32^3 \times 64$	0.0030	310	3.3	144	[16, 31]	[21, 31]
$C_2$				0.0060	430	4.6	128		
$C_3$				0.0080	500	5.3	128		

Table 1: Details of the ensembles of gauge configurations used in the present study: value of the gauge coupling  $\beta$ ; approximate value of the lattice spacing  $a$ ; lattice size  $V = L^3 \times T$  in lattice units; bare sea quark mass in lattice units; approximate value of the pion mass; approximate value of the product  $m_\pi L$ ; number of independent configurations  $N_{cfg}$ . We also provide the fitting time interval in lattice units chosen for the two-point pseudoscalar correlators in the pion and kaon sectors,  $(\Delta t)_{\pi,K}$ , and in the  $D$ -meson sectors,  $(\Delta t)_{D,D_s}$ .

	$A_2 - A_3$	$B_1 - B_4$	$B_7$	$B_6$	$C_1 - C_3$
$a\mu_l$	0.0080, 0.0110	0.0040, 0.0064, 0.0085, 0.0100	0.0030	0.0040	0.0030, 0.0060, 0.0080
$a\mu_s$	0.020, 0.025, 0.030, 0.036	0.022, 0.027, 0.032	0.022, 0.027	0.022, 0.027	0.015, 0.018 0.022, 0.026
$a\mu_c$	0.270, 0.310, 0.355, 0.435, 0.520	0.250, 0.320, 0.390, 0.460	0.250, 0.320	0.250, 0.320	0.200, 0.230, 0.260 0.315

Table 2: Values of simulated valence quark masses in lattice units for each configuration ensemble in the light, strange and charm sectors.

and other systematic uncertainties on the same data.<sup>1</sup>

With respect to our previous determination of  $f_\pi$  and  $f_K$  [4], the new ensembles used in the present analysis are those with  $\beta = 3.8$  ( $A_2$ - $A_3$ ) and  $\beta = 4.05$  ( $C_1$ - $C_3$ ) and the ensembles  $B_6$ - $B_7$  at  $\beta = 3.9$ . The ensemble  $B_7$  has the lightest simulated mass  $\mu_l \sim 0.15 m_s^{phys.}$ , where  $m_s^{phys.}$  is the physical strange quark mass. The ensembles  $B_1$  and  $B_6$  have the same value of  $\beta$  and sea quark mass but different volumes,  $L \simeq 2.0$  fm and  $L \simeq 2.7$  fm, thus allowing a study of finite size effects.

In order to investigate the properties of the  $\pi$ ,  $K$ ,  $D$  and  $D_s$  mesons, we simulate the sea and valence light ( $u/d$ ) quark mass in the range  $0.15 m_s^{phys.} \lesssim \mu_l \lesssim 0.5 m_s^{phys.}$ , the valence strange quark mass is within  $0.9 m_s^{phys.} \lesssim \mu_s \lesssim 1.5 m_s^{phys.}$ , and the valence charm quark mass within  $0.8 m_c^{phys.} \lesssim \mu_c \lesssim 1.5 m_c^{phys.}$ ,  $m_c^{phys.}$  being the physical charm mass. The values of the valence quark masses simulated for each configuration ensemble

<sup>1</sup>For the basic ideas of this analysis in the unitary case see ref. [23].

are collected in Table 2. These values can be converted into the corresponding values of the renormalized quark masses (e.g. in the  $\overline{\text{MS}}$  scheme) using the available determinations of renormalization constants given in refs. [24, 25].

As already noted, with twisted mass fermions at maximal twist, the determination of the pseudoscalar decay constants, besides being automatically improved at  $\mathcal{O}(a)$ , does not require the introduction of any renormalization constants. For a pseudoscalar meson of mass  $m_{PS}$ , composed of valence quarks with masses  $\mu_{val}^{(1)}$  and  $\mu_{val}^{(2)}$ , the decay constant  $f_{PS}$  is obtained as

$$f_{PS} = \left( \mu_{val}^{(1)} + \mu_{val}^{(2)} \right) \frac{|\langle 0|P|PS\rangle|}{m_{PS} \sinh m_{PS}}, \quad (1)$$

where  $P = \bar{q}_1 \gamma_5 q_2$ . The meson mass  $m_{PS}$  and the matrix element  $|\langle 0|P|PS\rangle|$  entering eq. (1) have been extracted from a single state fit of the two-point pseudoscalar correlation function within the time intervals collected in Table 1. The replacement of  $m_{PS}$  with  $\sinh m_{PS}$  in the lattice definition (1) of the decay constant helps in reducing discretization errors for heavy meson masses. Combined with the observation that the tree-level KLM factor for the quark field is equal to one for twisted mass fermions at maximal twist [14], this replacement allows to remove at tree level all  $\mathcal{O}((am_c)^n)$  terms in the determination of the  $D_{(s)}$ -meson decay constant.

The statistical accuracy of the meson correlators is improved by using the so-called “one-end” stochastic method, implemented in ref. [26] (see also [8]), which includes all spatial sources at a single timeslice. Statistical errors on the meson masses and decay constants are evaluated using the jackknife procedure, with 16 jackknife bins for each configuration ensemble. Statistical errors on the fit results which are based on data obtained from independent ensembles of gauge configurations are evaluated using a bootstrap procedure, with 100 bootstrap samples. In order to illustrate the quality of the data, we show in fig. 1 the effective masses of pseudoscalar mesons, as a function of the time, for four choices of quark mass combinations, representing the pion, the kaon, the  $D$  and  $D_s$  mesons, respectively. The pseudoscalar masses shown in fig. 1 are extracted from the two point correlator of the charged pseudoscalar density, together with the matrix element  $\langle 0|P|PS\rangle$ . Both quantities enter eq. (1) for  $f_{PS}$ . Each plot shows the effective mass obtained from the ensembles  $B_1$  and  $B_6$ , i.e. at  $\beta = 3.9$ , with  $a\mu_{sea} = 0.0040$  and with two different lattice sizes, namely  $24^3 \times 48$  and  $32^3 \times 64$  (see Sec. 3.1 for a discussion of finite size effects in our analysis).

## 3 The pion and kaon decay constants

### 3.1 Combined chiral and continuum extrapolation

A good convergence of SU(3)-ChPT is in general not guaranteed in the kaon sector. As recently pointed out in [20] (see also [27] for a detailed review on this subject), a safer approach consists in avoiding the chiral expansion in terms of the strange quark mass and applying therefore SU(2)-ChPT. The use of SU(2)-ChPT is well motivated in our analysis, since we simulated  $\mu_s$  in the range of the physical strange quark mass, thus having small values of  $\mu_l/\mu_s$  (see Table 2). At next-to-leading order (NLO), the SU(2)-ChPT prediction

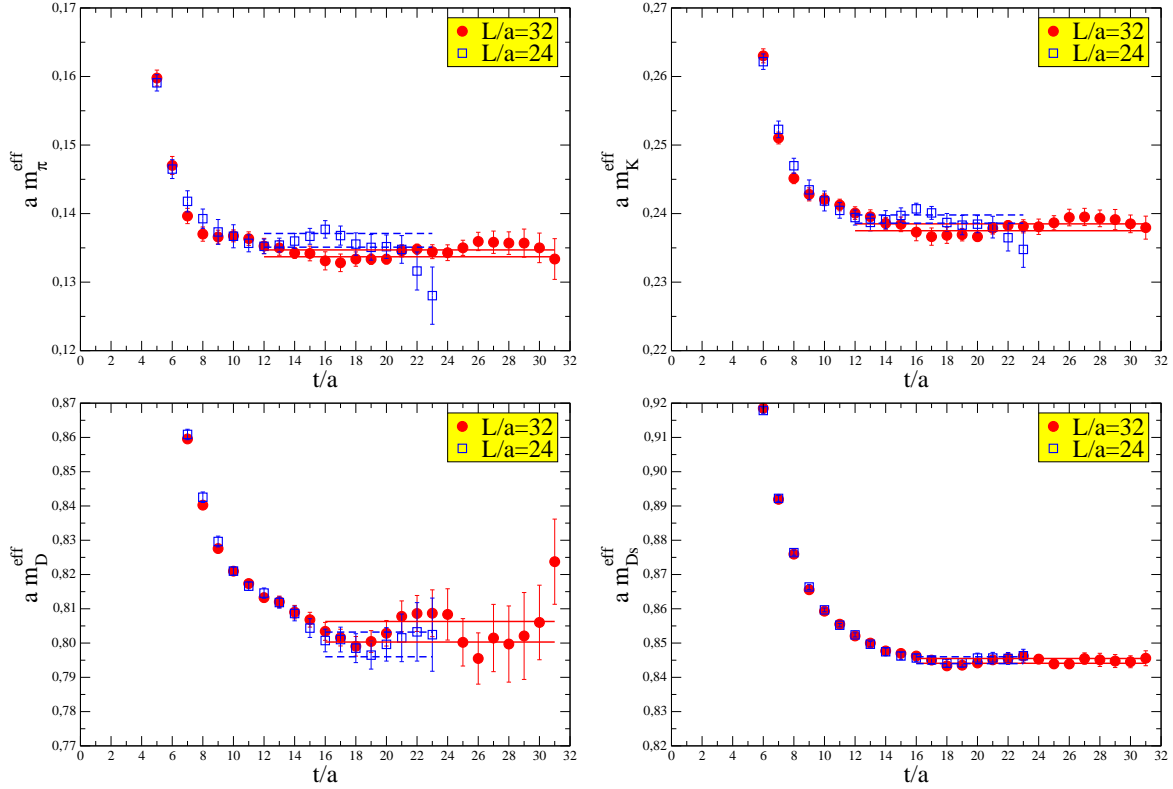


Figure 1: *Effective pseudoscalar meson masses  $m_{PS}^{eff}(a\mu_{sea}, a\mu_{val}^{(1)}, a\mu_{val}^{(2)})$  as a function of time, in lattice units, with  $\mu_{sea}$  and  $\mu_{val}^{(1,2)}$  denoting generically the sea and valence quark masses respectively. For illustrative purposes the following choices of quark mass combinations are displayed:  $m_{PS}(0.0040, 0.0040, 0.0040)$  (pion),  $m_{PS}(0.0040, 0.0040, 0.0220)$  (kaon),  $m_{PS}(0.0040, 0.0040, 0.2500)$  ( $D$ -meson),  $m_{PS}(0.0040, 0.0220, 0.2500)$  ( $D_s$ -meson). In each plot we compare the effective masses as obtained from the two ensembles  $B_1$  and  $B_6$ , which correspond to different lattice sizes. Dashed and solid lines represent the  $1\text{-}\sigma$  ranges of the corresponding masses as obtained from the fit of the two-point correlation functions.*

for the pion decay constant is well known [28],

$$f_{PS}(\mu_l, \mu_l, \mu_l) = f \cdot (1 - 2\xi_u \ln \xi_u + b\xi_u) , \quad (2)$$

and the corresponding expression for the kaon decay constant reads [20]

$$f_{PS}(\mu_l, \mu_l, \mu_s) = f^{(K)} \cdot \left(1 - \frac{3}{4}\xi_u \ln \xi_u + b^{(K)}\xi_u\right) . \quad (3)$$

We are using the notation  $(\mu_{sea}, \mu_{val}^{(1)}, \mu_{val}^{(2)})$  for the quark mass content of the corresponding meson, and the variables  $\xi$ 's in eqs. (2) and (3) are expressed in our analysis as a function of meson masses,<sup>2</sup>

$$\xi_{ij} = \frac{m_{PS}^2(\mu_l, \mu_i, \mu_j)}{(4\pi f)^2} . \quad (4)$$

<sup>2</sup>We use the normalization in which  $f_\pi = 130.7$  MeV.

The leading contribution in eq. (2) is represented by the low energy constant (LEC)  $f$ , which provides the value of the pion decay constant in the chiral limit, whereas the coefficient  $b$  is related to the LEC  $\bar{l}_4$  of the NLO chiral Lagrangian. Notice that, in the  $N_f = 2$  theory we are simulating, i.e. with a quenched strange quark, these constants are independent of the value of the strange quark mass. In this theory there is actually no distinction between SU(2) and SU(3) ChPT expansions for pion observables. The LECs  $f^{(K)}$  and  $b^{(K)}$  entering the SU(2) formula (3) for the kaon decay constant, instead, are functions of the (valence) strange quark mass.

In order to perform a combined fit of the data for the pseudoscalar decay constants at the three values of the lattice spacing, we rely on the Symanzik expansion of the lattice regularized theory and introduce in the fitting formulae discretization terms of  $\mathcal{O}(a^2)$  and  $\mathcal{O}(a^2 \mu_s)$ . Discretization effects of  $\mathcal{O}(a^2 \mu_l)$ , i.e. proportional to the light quark mass, represent very small contributions that turn out to be invisible in the fit. Moreover, since the simulated  $\mu_s$  masses are all close to the physical strange quark mass, we can safely linearize the strange mass dependence of the LECs  $f^{(K)}$  and  $b^{(K)}$  in eq. (3) around  $m_s^{phys.}$ . We thus write the SU(2)-ChPT fitting formulae for the pion and kaon decay constants as

$$f_{PS}(\mu_l, \mu_l, \mu_l) = f \cdot \left( 1 - 2 \xi_{ll} \ln \xi_{ll} + b \xi_{ll} + A \frac{a^2}{r_0^2} \right), \quad (5)$$

$$f_{PS}(\mu_l, \mu_l, \mu_s) = (f_0^{(K)} + f_m^{(K)} \xi_{ss}) \cdot \left[ 1 - \frac{3}{4} \xi_{ll} \ln \xi_{ll} + (b_0^{(K)} + b_m^{(K)} \xi_{ss}) \xi_{ll} + (A_a + A_{as} \xi_{ss}) \frac{a^2}{r_0^2} \right]. \quad (6)$$

The fit is performed in units of the Sommer parameter  $r_0$  [29]. The values of  $r_0/a$  at the three lattice spacings have been extracted in ref. [9] from the analysis of the static potential, obtaining

$$r_0/a = \{4.46(3), 5.22(2), 6.61(3)\} \quad (7)$$

at  $\beta = \{3.8, 3.9, 4.05\}$  respectively. The physical value of  $r_0$  in the continuum limit is determined in our analysis by combining the determination of  $r_0 \cdot f_\pi$  with the experimental value of the pion decay constant. This procedure, combined with eq. (7), corresponds to fixing the lattice scale using  $f_\pi$  as physical input.

An important ingredient in the analysis is the study of finite size effects (FSE). With our simulation setup, the largest FSE are expected in the data of the ensembles  $B_1$  and  $C_1$ , for which  $m_\pi L \simeq 3.3$  (see Table 1). A quantitative estimate of these effects can be obtained from the comparison of the data of the ensembles  $B_1$  and  $B_6$ , that only differ in lattice size. This comparison provides consistent results with the FSE predicted at NLO by SU(2)-ChPT [30, 31], which are expressed for the pion and kaon decay constants by

$$\begin{aligned} f_{PS}(\mu_l, \mu_l, \mu_l; L) &= f_{PS}(\mu_l, \mu_l, \mu_l) \cdot [1 - 2 \xi_{ll} \tilde{g}_1(L, \xi_{ll})], \\ f_{PS}(\mu_l, \mu_l, \mu_s; L) &= f_{PS}(\mu_l, \mu_l, \mu_s) \cdot \left[ 1 - \frac{3}{4} \xi_{ll} \tilde{g}_1(L, \xi_{ll}) \right], \end{aligned} \quad (8)$$

where the function  $\tilde{g}_1$  is defined for instance in ref. [4].<sup>3</sup> This correction, which on the ensembles  $B_1$  and  $C_1$  corresponds to about 2.5% for  $f_\pi$  and 0.9% for  $f_K$ , has been included

---

<sup>3</sup>Note that the finite size corrections in eq. (8) are obtained from the loop contribution of the infinite volume ChPT predictions in eqs. (2) and (3) by replacing  $\ln \xi$  with the function  $\tilde{g}_1(L, \xi)$ .



$r_0 \cdot f$	$r_0 \cdot f_0^{(K)}$	$r_0 \cdot f_m^{(K)}$	$b$	$b_0^{(K)}$	$b_m^{(K)}$	$A$	$A_a$	$A_{as}$
0.271(6)	0.305(6)	0.18(1)	-0.25(13)	0.5(1)	-1.9(4)	0.7(5)	0.7(4)	2.1(6)
0.274(9)	0.312(9)	0.18(2)	-0.33(15)	0.4(2)	-1.7(5)	0.5(7)	0.3(7)	3(1)

Table 3: Values of the  $SU(2)$  fit parameters of eqs. (5) and (6), as obtained by including (first row) or excluding (second row) the data at  $\beta = 3.8$ . Quoted errors are statistical plus fitting errors.

		$r_0$ [GeV $^{-1}$ ]	$f_K$ [MeV]	$f_K/f_\pi$	$\chi^2/dof$
SU(2)-ChPT	incl. $\beta = 3.8$	2.22(5)	158.1(8)	1.210(6)	{11/8; 40/30}
	excl. $\beta = 3.8$	2.25(7)	158.9(1.4)	1.216(11)	{7/6; 35/22}
SU(3)-ChPT	incl. $\beta = 3.8$	2.23(5)	158.2(6)	1.210(5)	61/42
	excl. $\beta = 3.8$	2.28(7)	158.0(0.8)	1.209(6)	54/32

Table 4: Values of  $r_0$ ,  $f_K$  and  $f_K/f_\pi$  as obtained from  $SU(2)$ - and  $SU(3)$ -ChPT by including or excluding the data at  $\beta = 3.8$ . For each fit, the chi-squared per degree of freedom,  $\chi^2/dof$ , is also given in the last column. For fits based on  $SU(2)$ -ChPT, the two values of  $\chi^2/dof$  correspond to the fit of  $f_\pi$  and  $f_K$  respectively. Quoted errors are statistical plus fitting errors.

in our fit. For a more detailed discussion of FSE in the pion decay constant see ref. [8]. In our data for the kaon decay constant, instead, the differences between the ensembles  $B_1$  and  $B_6$  are small and at the level of the statistical errors. We obtain  $\Delta_{f_K} \equiv f_K^{L=24}/f_K^{L=32} - 1 = 0.005(4)$ , compatible with zero. Also the NLO partially quenched ChPT prediction for  $\Delta_{f_K}$  [31] is similarly small ( $-0.006$ ), at the level of our statistical error.

The values of the fit parameters and the results for  $r_0$ ,  $f_K$  and  $f_K/f_\pi$  are collected in Tables 3 and 4, respectively. The extrapolation to the physical up/down quark mass and the interpolation to the physical strange mass has been performed by inserting in eqs. (5) and (6)  $\xi_{ll} = (m_\pi^{phys.})^2/(4\pi f)^2$  and  $\xi_{ss} = (2(m_K^{phys.})^2 - (m_\pi^{phys.})^2)/(4\pi f)^2$ , where  $m_\pi^{phys.}$  and  $m_K^{phys.}$  are the experimental pion and kaon masses. In both Tables, we show the results of our fits when we take the data at  $\beta = 3.8$  into account and when we leave them out. As can be seen, the values of the fit parameters, as well as those of the decay constants, are found to be well consistent in the two cases. In the following, therefore, we will consider for  $f_K$  and  $f_K/f_\pi$  only the predictions obtained by including the  $\beta = 3.8$  data. From the results given in Tables 3 and 4, one can also derive our prediction for the pion decay constant in the chiral limit,  $f$ , and the LEC  $\bar{l}_4 = b/2 + 2\ln(4\pi f/m_{\pi^+})$ . We obtain the values  $f = 121.7(1)\text{MeV}$  and  $\bar{l}_4 = 4.66(6)$ , which are in good agreement with the results of the scaling analysis performed by our Collaboration in [10],  $f = 121.66(7)(26)\text{MeV}$  and  $\bar{l}_4 = 4.59(4)(13)$ . The quality of the fit for the combined chiral and continuum extrapolation of the pion and kaon decay constant is illustrated in fig. 2.

As an alternative to the  $SU(2)$ -ChPT approach, we have also considered the expansion valid for a small strange quark mass, fitting both the pion and the kaon decay constants using  $SU(3)$ -ChPT. The relevant expression, valid for the partially quenched  $N_f = 2$  theory

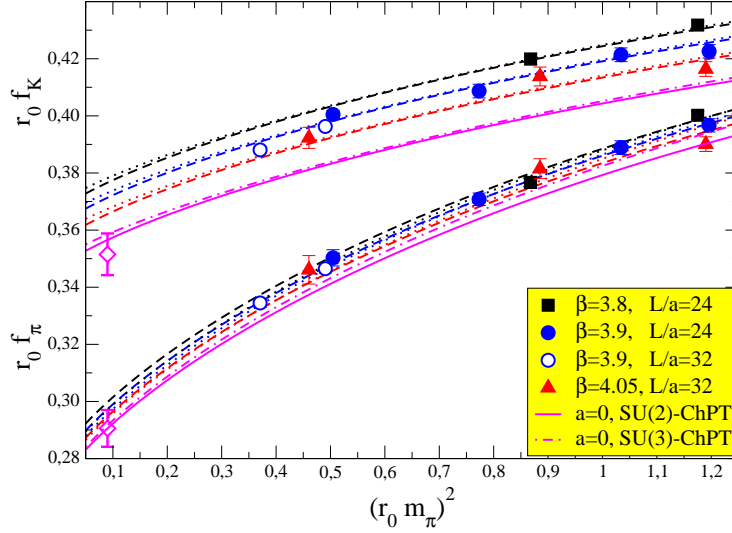


Figure 2: Lattice results for  $r_0 f_\pi \equiv r_0 f_{PS}(\mu_l, \mu_l, \mu_l)$  and  $r_0 f_K \equiv r_0 f_{PS}(\mu_l, \mu_l, \mu_s)$  as a function of the pion mass square  $(r_0 m_\pi)^2 \equiv (r_0 m_{PS}(\mu_l, \mu_l, \mu_l))^2$ . For the kaon, we display data with  $\mu_s$  fixed to the simulated mass that corresponds to a reference meson mass  $r_0 m_{PS}(\mu_l, \mu_s, \mu_s) \simeq 1.63$ . The SU(2)- (SU(3)-) ChPT extrapolation to the physical pion mass is represented at fixed lattice spacing by the dashed (dotted) curves, and in the continuum limit by the solid (dashed-dotted) curve. Our results for the physical values of the pion and kaon decay constants, obtained from SU(2)-ChPT, are illustrated by diamonds in the plot. In the kaon case an interpolation to the physical strange quark mass is performed.

at NLO, is [32]

$$f_{PS}(\mu_l, \mu_l, \mu_s) = f \cdot \left[ 1 - \frac{3}{4} \xi_{ll} \ln \xi_{ll} - \frac{\xi_{ll}}{4} \ln \xi_{ss} - \xi_{ls} \ln \xi_{ls} + b_{ll} \xi_{ll} + b_{ss} \xi_{ss} + (B_a + B_{as} \xi_{ss}) \frac{a^2}{r_0^2} \right], \quad (9)$$

where, as in the SU(2) case, we have also included in the fit discretization terms of  $\mathcal{O}(a^2)$  and  $\mathcal{O}(a^2 \mu_s)$  as well as finite size corrections [31].

The results obtained from the SU(3)-ChPT analysis are given in Table 4 and shown in fig. 2, and are found in very good agreement with those obtained from the SU(2) fit. A more careful analysis suggests, however, that the SU(3)-ChPT fit is less robust than the one based on SU(2). In SU(2)-ChPT, at NLO, one obtains a good fit of the data by expressing the chiral formulae (5) and (6) either in terms of meson masses, as performed here with  $\xi_{ij}$  defined as in eq. (4), or in terms of quark masses, i.e. with  $\xi_{ij} = B(\mu_i + \mu_j)/(4\pi f)^2$ , where  $B$  is the LEC entering at LO in the chiral Lagrangian. In SU(3)-ChPT, instead, the NLO formula expressed in terms of meson masses provides a good description of the lattice data, but fits performed in terms of quark masses require in the kaon sector the inclusion of NNLO terms, as we already found in [4]. This means that the replacement of quark with meson masses effectively resums higher order chiral contributions, actually improving the fit based on NLO SU(3)-ChPT of the pseudoscalar decay constant beyond  $m_{PS} \sim 450$  MeV. A similar result was found in ref. [33].

### 3.2 Results for $f_K$ and $f_K/f_\pi$

As seen in the previous section, lattice data in the kaon sector could be analysed by means of either SU(2)- or SU(3)-ChPT, leading to almost identical results, see Table 4. The results we quote for  $f_K$  and  $f_K/f_\pi$  are those obtained from SU(2). The errors quoted in Table 4 are statistical plus fitting errors from the combined chiral and continuum extrapolation. We now discuss how we evaluate other systematic errors.

Since we have simulated at three values of the lattice spacing and on our coarsest lattice ( $\beta = 3.8$ ) we have data for only two values of the light quark mass, we include in our final results a systematic uncertainty due to residual discretization effects. The leading discretization errors in our determination of the light meson decay constants are expected to be of  $\mathcal{O}(a^2 \Lambda_{QCD}^2)$ . This naïve expectation is roughly confirmed by the results of our fit. On our finest lattice, for instance, with  $\beta = 4.05$  and  $a \simeq 0.07$  fm, one has  $a^2 \Lambda_{QCD}^2 \simeq 1 \div 2\%$  and we find that the difference between the values taken by the kaon decay constant on this lattice and its estimate in the continuum limit is approximately 2.6% (this difference turns out to be slightly larger, about 2.8%, at the reference mass  $r_0 m_{PS}(\mu_l, \mu_s, \mu_s) = 1.63$  for which results are displayed in fig. 2). We conservatively assume an error of 50% in the continuum extrapolation starting from the data on our finest lattice, thus adding to our final results for  $f_K$  and  $f_K/f_\pi$  a relative systematic error of 1.3% (half of the difference between the values at  $\beta = 4.05$  and the continuum estimates).

In the present analysis, FSE corrections have been implemented by using the predictions of NLO ChPT, as discussed in the previous section. Besides the direct comparison of this theoretical estimate with the data available on the two lattices  $B_1$  and  $B_6$ , where  $m_\pi L$  varies from 3.3 to 4.3, an additional indication that these corrections are under control is provided by the compatibility between the results for  $f_\pi$  determined here, by treating the FSE with NLO ChPT, and those obtained in [8] by using the resummed formulae of ref. [34]. For the kaon decay constant, FSE are found at the level of the statistical errors at most. A fit performed without including this correction provides a result for the kaon decay constant which is lower by about 0.7%. We conservatively include this difference in the systematic error of  $f_K$  as an estimate of the uncertainty due to FSE.

The only uncertainty which cannot be reliably estimated within our  $N_f = 2$  simulation, is the error due to the quenching of the strange quark. The good agreement observed among the recent  $N_f = 2$  and  $N_f = 2 + 1$  lattice determinations of  $f_K$  and  $f_K/f_\pi$  (see fig. 3) suggests, however, that such an effect is smaller than the other systematic uncertainties estimated above. The ETM Collaboration is planning to investigate directly the effect of the quenching of both the strange and charm quarks through simulations with  $N_f = 2 + 1 + 1$ , which are currently in progress [35]. For a more extensive discussion of the various sources of lattice systematic uncertainties see ref. [36].

Our final results for the kaon decay constant and the ratio  $f_K/f_\pi$  are then

$$f_K = 158.1(0.8)(2.0)(1.1) \text{ MeV} \quad , \quad f_K/f_\pi = 1.210(6)(15)(9) \quad , \quad (10)$$

where the first error comes from statistics and chiral extrapolation, the second from the estimate of residual discretization effects and the third from the uncertainty on FSE cor-

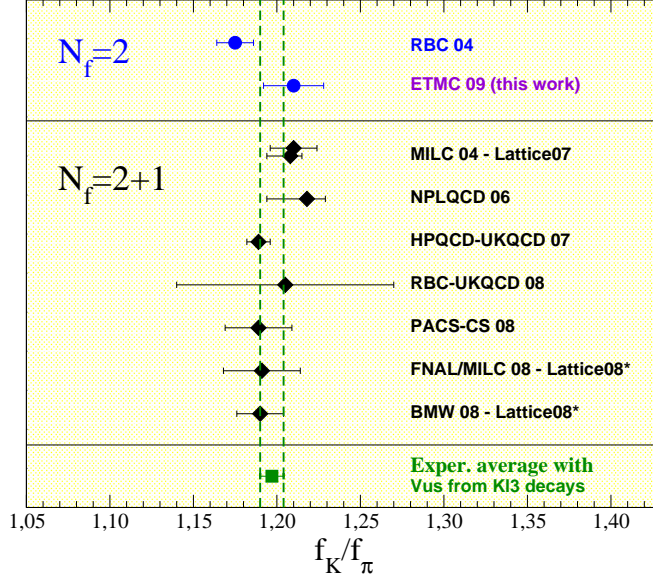


Figure 3: *Lattice QCD determinations of the ratio  $f_K/f_\pi$  obtained from simulations with  $N_f = 2$  [37] and  $N_f = 2+1$  [20, 27], [37]-[43] dynamical quarks. A star in the legend denotes preliminary results. The results are also compared with the experimental average of  $f_K/f_\pi$  obtained by using for  $V_{us}$  the determination from  $K_{\ell 3}$  decays [44].*

rections. By combining the errors in quadrature, we finally obtain

$$f_K = 158.1(2.4) \text{ MeV} \quad , \quad f_K/f_\pi = 1.210(18) . \quad (11)$$

Our result for the ratio  $f_K/f_\pi$  is compared in fig. 3 with other unquenched lattice determinations, performed with either  $N_f = 2$  or  $N_f = 2 + 1$  dynamical quarks, as well as with the experimental average of  $f_K/f_\pi$  obtained by using for  $V_{us}$  the determination from  $K_{\ell 3}$  decays [44]. Our result turns out to be in very good agreement with the latter determination, as well as with most of the  $N_f = 2$  and  $N_f = 2 + 1$  lattice results.

Alternatively, our result for  $f_K/f_\pi$  can be combined with the experimental measurement of  $\Gamma(K \rightarrow \mu\bar{\nu}_\mu(\gamma))/\Gamma(\pi \rightarrow \mu\bar{\nu}_\mu(\gamma))$  [44] to get a determination of the ratio  $|V_{us}|/|V_{ud}|$  [1]. We obtain

$$|V_{us}|/|V_{ud}| = 0.2281(5)(35) , \quad (12)$$

where the first error is the experimental one and the second is the theoretical error coming from the uncertainty on  $f_K/f_\pi$ . Eq. (12), combined with the determination  $|V_{ud}| = 0.97425(22)$  [45] from nuclear beta decays, yields the estimate

$$|V_{us}| = 0.2222(5)(34) , \quad (13)$$

in good agreement, though with a larger error, with the value extracted from  $K_{\ell 3}$  decays,  $|V_{us}| = 0.2246(12)$  [44]. Eq. (13) and the value of  $|V_{ud}|$  quoted above leads to

$$|V_{ud}|^2 + |V_{us}|^2 + |V_{ub}|^2 - 1 = -1.5(1.6) \cdot 10^{-3} . \quad (14)$$

in good agreement with the unitarity constraint of the CKM matrix.

## 4 The $D$ and $D_s$ decay constants

### 4.1 Combined chiral and continuum extrapolation

In order to determine the  $D$  and  $D_s$  meson decay constants we essentially proceed as in the kaon sector. We analyse simultaneously data at the three values of the lattice spacing and perform for the pseudoscalar decay constants combined fits of the meson mass dependence and of discretization effects. The simulated values  $\mu_c$  of the charm quark mass are close to the physical charm quark mass ( $0.8 m_c^{phys.} \lesssim \mu_c \lesssim 1.5 m_c^{phys.}$ ), so that the interpolation to the physical value is short and smooth. From the comparison of the data of the ensembles  $B_1$  and  $B_6$  we also find that FSE are negligible for the  $D_s$  decay constants, and they are at the level of the statistical error or smaller for  $f_D$ . On the other hand, discretization errors induced by the charm quark mass have to be taken carefully into account in the fit, being parametrically of  $\mathcal{O}(a^2 \mu_c^2)$ , i.e. approximately  $5 \div 10\%$  in our simulation.

The functional forms describing the mass dependence of the decay constants assumed to fit the data in the  $D$  and  $D_s$  sectors are those predicted by HMChPT [19]. We consider the SU(2) version of the theory, as in the case of the kaon sector, where the strange quark is not required to satisfy chiral symmetry, but it is considered heavy enough to justify an expansion in powers of  $\mu_l/\mu_s$ . For comparison, we have also investigated the predictions of SU(3)-HMChPT where, instead, the strange quark is required to satisfy the same chiral symmetry of the light up and down quarks. As we will see below, in the  $D$ -meson sector the SU(2)-HMChPT approach turns out to work significantly better than the one based on SU(3).

Within the SU(2)-HMChPT analysis, we extract  $f_D$  and  $f_{D_s}$  by considering two different procedures. In the first one we fit the two following combinations of meson masses and decay constants:

$$f_{D_s} \sqrt{m_{D_s}}, \quad R \equiv \frac{f_{D_s} \sqrt{m_{D_s}}}{f_D \sqrt{m_D}}, \quad (\text{Fit I}) . \quad (15)$$

We find, in particular, that the advantage of introducing the ratio  $R$  is that discretization effects largely cancel in the ratio. In the second approach we consider the previous quantities divided by the light decay constants, i.e. we fit the ratios

$$R_1 \equiv \frac{f_{D_s} \sqrt{m_{D_s}}}{f_K}, \quad R_2 \equiv \frac{f_{D_s} \sqrt{m_{D_s}}}{f_K} \times \frac{f_\pi}{f_D \sqrt{m_D}} . \quad (\text{Fit II}) \quad (16)$$

Here, the advantage of the ratio  $R_2$  is that it exhibits a quite smooth chiral behaviour. The comparison of the results obtained for  $f_D$ ,  $f_{D_s}$  and  $f_{D_s}/f_D$  in the two cases, Fit I and Fit II, will provide an estimate of the systematic uncertainty due to the chiral extrapolation.

In all quantities entering eqs. (15) and (16), the  $D$ -mesons decay constants are multiplied by the square roots of the corresponding meson masses, in order to reconstruct the observables that remain finite in the infinite mass limit. The Heavy Quark Effective Theory predicts in fact for a Heavy( $H$ )-light( $l$ ) meson an expansion of the form  $f_{Hl} \sqrt{m_{Hl}} = A + B/m_{Hl} + \mathcal{O}(1/m_{Hl}^2)$ , up to small radiative corrections. Though the heavy quark expansion is known to be slowly convergent in the charm mass region, in our analysis we can safely assume such a behaviour for the  $D$  mesons since only a short

interpolation of the lattice data to the physical charm quark mass is needed. Moreover, since the contribution of the sub-leading  $1/m_{Hl}$  correction in this interpolation is small, we can safely account for the dependence on the light meson masses only in the leading term, by using the prediction of HMChPT.

We obtain the SU(2)-HMChPT functional forms for the quantities in eqs. (15) and (16) by expanding the corresponding SU(3)-HMChPT predictions in powers of  $\mu_l/\mu_s$ , and re-absorbing the strange quark mass dependence in the SU(2) LECs.<sup>4</sup> The SU(3)-HMChPT prediction for  $f_{D_s}\sqrt{m_{D_s}}$ , valid in the partially quenched  $N_f = 2$  theory [19], is given by

$$f_{D_s}\sqrt{m_{D_s}} = \frac{C_1}{r_0^{3/2}} \left[ 1 - \frac{1 + 3g_c^2}{2} \left( 2\xi_{ls} \ln \xi_{ls} + \frac{\xi_{lu} - 2\xi_{ls}}{2} \ln \xi_{ss} \right) + C_2\xi_{lu} + C_3\xi_{ss} \right] + \frac{C_4}{r_0^{5/2}m_{D_s}}, \quad (17)$$

where the parameter  $g_c$  is related to the  $g_{D^*D\pi}$  coupling by  $g_{D^*D\pi} = (2\sqrt{m_D m_{D^*}}/f_\pi) g_c$ . Since eq. (17) does not contain logarithms of the pion mass (i.e.  $\ln \xi_{ll}$ ), one finds that its expansion in powers of  $\mu_l/\mu_s \simeq \xi_{lu}/\xi_{ss}$  leads to an SU(2) chiral expression for the  $D_s$  decay constant which is free of chiral logarithms at NLO. As in the light meson case, we also include in the fitting formula discretization terms of  $\mathcal{O}(a^2)$ , in order to take simultaneously into account the lattice artefacts. We observe, in this respect, that the Symanzik expansion of  $f_D$  and  $f_{D_s}$  contains at  $\mathcal{O}(a^2)$  discretization terms depending on the charm quark mass either linearly or quadratically, with the leading contribution expected from terms of  $\mathcal{O}(a^2 \mu_c^2)$ . The limited set of data available in our analysis, however, does not allow us to fit both these dependencies separately. We parameterize these discretization effects in terms of the meson masses, and we thus introduce in the fitting formula only a term proportional to  $a^2 m_{D_s}^2$ . We have also tried an alternative fit where the charm mass dependent discretization term is taken to be proportional to  $a^2 m_{D_s}$  instead of  $a^2 m_{D_s}^2$ , and we obtain completely consistent results. Thus, we use as our fitting formula for  $f_{D_s}\sqrt{m_{D_s}}$  the expression

$$f_{D_s}\sqrt{m_{D_s}} = \frac{D_1}{r_0^{3/2}} \left[ 1 + D_2\xi_{lu} + (D_a + D_{as}\xi_{ss}) \frac{a^2}{r_0^2} + D_{ah} a^2 m_{D_s}^2 \right] + \frac{D_3}{r_0^{5/2}m_{D_s}}, \quad (18)$$

where the coefficients  $D_1$  and  $D_2$ , which depend on the strange quark mass, are expressed in the fit as linear functions of this mass:

$$D_i = D_{i,0} + D_{i,m} \xi_{ss}, \quad (19)$$

with  $i = 1, 2$ .

The SU(2)-HMChPT prediction for the ratio  $R$ , defined in eq. (15), is straightforwardly obtained by dividing eq. (18) by the HMChPT expression for  $f_D\sqrt{m_D}$ , which is provided by the SU(3)-HMChPT formula of eq. (17) with  $\mu_s = \mu_l$ . Thus, we assume for the ratio  $R$  the expression

$$R = D'_1 \left[ 1 + \frac{3}{4} (1 + 3g_c^2) \xi_{lu} \ln \xi_{lu} + D'_2\xi_{lu} + (D'_a + D'_{as}\xi_{ss}) \frac{a^2}{r_0^2} + D'_{ah} a^2 m_{D_s}^2 \right] + \frac{D'_3}{r_0 m_{D_s}}, \quad (20)$$

---

<sup>4</sup>The same procedure allows to obtain the SU(2)-ChPT expression (3) of the kaon decay constant  $f_K$  from the SU(3) prediction of eq. (9).

$D_{1,0}$	$D_{1,m}$	$D_{2,0}$	$D_{2,m}$	$D_3$	$D_a$	$D_{as}$	$D_{ah}$
1.62(9)	0.78(7)	0.4(2)	-0.7(5)	-2.9(3)	-0.2(4)	-2(1)	0.13(3)
1.54(9)	0.9(1)	0.7(2)	-1.3(5)	-2.6(3)	-0.6(7)	-3(2)	0.16(2)
$D'_{1,0}$	$D'_{1,m}$	$D'_{2,0}$	$D'_{2,m}$	$D'_3$	$D'_a$	$D'_{as}$	$D'_{ah}$
1.0(1)	1.1(2)	1.9(4)	-2.1(9)	0.6(4)	-1.4(9)	0(1)	0.07(5)
1.0(1)	1.2(2)	2.1(6)	-3(1)	0.5(6)	-1(1)	1(2)	0.07(7)

$P_{1,0}$	$P_{1,m}$	$P_{2,0}$	$P_{2,m}$	$P_3$	$P_a$	$P_{as}$	$P_{ah}$
4.9(2)	0.7(2)	0.7(2)	0.1(5)	-7.2(8)	-0.1(4)	-3(1)	0.11(2)
4.7(2)	0.8(3)	0.9(2)	-0.5(5)	-6.8(7)	-0.2(6)	-4(2)	0.12(2)
$P'_{1,0}$	$P'_{1,m}$	$P'_{2,0}$	$P'_{2,m}$	$P'_3$	$P'_a$	$P'_{as}$	$P'_{ah}$
0.9(1)	0.4(1)	0.9(5)	-2(1)	0.4(4)	-2(1)	-1(2)	0.08(5)
0.9(1)	0.4(1)	0.9(6)	-3(2)	0.3(5)	-1(2)	1(3)	0.06(7)

Table 5: Values of the SU(2)-HMChPT fit parameters from Fit I of eqs. (18) and (20) (upper table) and from Fit II of eq. (21) (lower table), as obtained by including (first row) or excluding (second row) the data at  $\beta = 3.8$ . Quoted errors are statistical plus fitting errors.

where the coefficients  $D'_1$  and  $D'_2$  are expanded as linear functions of the strange quark mass as in eq. (19).

We find that the HMChPT parameter  $g_c$  cannot be determined from the fit, which is almost insensitive to it. It is thus constrained to the experimental value  $g_c = 0.61(7)$  [2, 46] which is in good agreement with a recent unquenched lattice determination,  $g_c = 0.71(7)$  [47].

The values of the coefficients  $D_i$  and  $D'_i$  as resulting from the fits of eqs. (18) and (20) are collected in Table 5. Using these results and inserting in eqs. (18) and (20) the experimental values of the relevant meson masses we obtain for  $f_D$ ,  $f_{D_s}$  and  $f_{D_s}/f_D$  the results given in Table 6 labelled as SU(2)-HMChPT, Fit I. As in the light meson case, we show in the Tables the results obtained by including or excluding the data at  $\beta = 3.8$ . The values of the fit parameters are consistent in the two cases and the results for the decay constants are essentially equal.

The alternative approach we considered to determine the  $D$  and  $D_s$  meson decay constants is based on the study of the ratios  $R_1$  and  $R_2$  defined in eq. (16). The SU(2)-HMChPT predictions for these ratios are easily obtained by dividing the expressions (18) and (20) for  $f_{D_s}\sqrt{m_{D_s}}$  and  $R$  by the SU(2)-ChPT predictions (2) and (3) for  $f_\pi$  and  $f_K$ , corrected for FSE as in eq. (8). The resulting expressions read

$$R_1 = \frac{P_1}{r_0^{1/2}} \left[ 1 + \frac{3}{4} \xi_u \ln \xi_u + P_2 \xi_u + (P_a + P_{as} \xi_{ss}) \frac{a^2}{r_0^2} + P_{ah} a^2 m_{D_s}^2 \right] + \frac{P_3}{r_0^{3/2} m_{D_s}}, \quad (21)$$

$$R_2 = P'_1 \left[ 1 + \left( \frac{3}{4} (1 + 3g_c^2) - \frac{5}{4} \right) \xi_u \ln \xi_u + P'_2 \xi_u + (P'_a + P'_{as} \xi_{ss}) \frac{a^2}{r_0^2} + P'_{ah} a^2 m_{D_s}^2 \right] + \frac{P'_3}{r_0 m_{D_s}},$$

where the coefficients  $P_1$ ,  $P_2$ ,  $P'_1$  and  $P'_2$  are then expressed as linear functions of the strange quark mass as in eq. (19).

		$f_D$ [MeV]	$f_{D_s}$ [MeV]	$f_{D_s}/f_D$	$\chi^2/dof$
SU(2)-HMChPT Fit I	incl. $\beta = 3.8$	195(6)	242(3)	1.24(3)	{93/136; 61/136}
	excl. $\beta = 3.8$	194(8)	239(5)	1.23(4)	{25/96; 49/96}
SU(2)-HMChPT Fit II	incl. $\beta = 3.8$	199(6)	246(3)	1.24(3)	{146/136; 69/136}
	excl. $\beta = 3.8$	195(8)	243(5)	1.24(5)	{24/96; 39/96}
SU(3)-HMChPT	incl. $\beta = 3.8$	197(6)	239(3)	1.22(2)	371/179

Table 6: Values of  $f_D$ ,  $f_{D_s}$  and  $f_{D_s}/f_D$  as obtained from the SU(2)-HMChPT Fits I and II by including or excluding data at  $\beta = 3.8$ . We also show in the last row the results obtained by fitting both  $f_{D_s}\sqrt{m_{D_s}}$  and  $f_D\sqrt{m_D}$  with their common SU(3)-HMChPT functional form. For each fit, the chi-squared per degree of freedom is given in the last column. For fits based on SU(2)-HMChPT, two values of  $\chi^2/dof$  are displayed, corresponding to  $f_{D_s}$  and  $R$  for Fit I or  $R_1$  and  $R_2$  for Fit II. Quoted errors are statistical plus fitting errors.

The values of the coefficients  $P_i$  and  $P'_i$  are collected in Table 5 and the results for  $f_D$ ,  $f_{D_s}$  and  $f_{D_s}/f_D$  are compared to those obtained from Fit I in Table 6. The two fits yield results that are in good agreement and with very similar uncertainties.

In fig. 4 we show the dependence on the pion mass square of the four quantities studied in Fits I and II. We observe that  $f_{D_s}\sqrt{m_{D_s}}$  (top-left) has a very mild dependence on  $m_\pi^2$ , in agreement with the SU(2)-HMChPT prediction of eq. (18) according to which chiral logarithms are absent for this quantity at NLO. The logarithmic dependence in  $f_{D_s}\sqrt{m_{D_s}}/f_K$  (top-right), thus comes only from the chiral logarithms predicted by SU(2)-ChPT for the kaon decay constant, see eq. (3). The lattice results for the double ratio  $(f_{D_s}\sqrt{m_{D_s}}/f_K)/(f_D\sqrt{m_D}/f_\pi)$  (bottom-right) are almost independent of the light quark mass. This is not unexpected, since the chiral logarithms largely cancel in the ratio. We also note that in the ratios  $R$  and  $R_2$  (bottom plots), where  $f_{D_s}\sqrt{m_{D_s}}$  is divided by  $f_D\sqrt{m_D}$ , discretization effects turn out to be negligible, smaller than the statistical uncertainties.

As done for the light mesons decay constants, as an alternative to the SU(2)-HMChPT approach, we have also tried to fit both the  $D$  and the  $D_s$  decay constants using SU(3)-HMChPT. The corresponding fitting formula is given by eq. (17) with the addition of discretization terms. As for the SU(2) case, we have tried two different fits, in which  $f_D\sqrt{m_D}$  and  $f_{D_s}\sqrt{m_{D_s}}$  are either divided or not by the light decay constants  $f_\pi$  and  $f_K$ . At variance with our results for the light meson sector, we find that the quality of the SU(3) fits, with  $\chi^2/dof \gtrsim 2$ , is worse than in the SU(2) case. For illustration, we show the results obtained from the SU(3)-HMChPT analysis in the last line of Table 6 (for the case in which the light decay constants are not introduced in the ratios) and in fig. 4. Even though these results are consistent with those obtained from SU(2)-HMChPT, given the poor quality of the SU(3) fits, they are not considered in deriving the final results.

## 4.2 Results for $f_D$ , $f_{D_s}$ and $f_{D_s}/f_D$

The results presented in Table 6 show that the SU(2)-HMChPT analyses based on Fits I and II lead to determinations of  $f_D$ ,  $f_{D_s}$  and  $f_{D_s}/f_D$  that are in very good agreement, with very similar statistical uncertainties. We choose to average these results and to quote



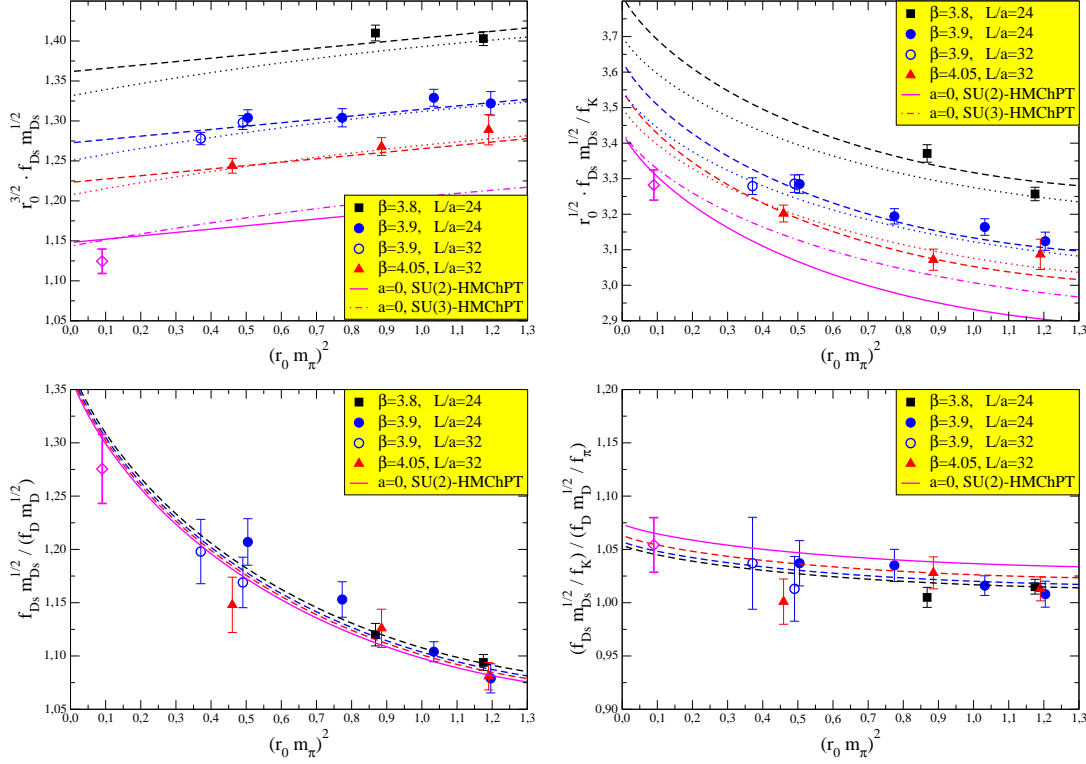


Figure 4: From top-left to bottom-right: lattice results for  $f_{D_s} \sqrt{m_{D_s}}$ ,  $R_1 = f_{D_s} \sqrt{m_{D_s}} / f_K$ ,  $R = f_{D_s} \sqrt{m_{D_s}} / (f_D \sqrt{m_D})$  and  $R_2 = (f_{D_s} \sqrt{m_{D_s}} / f_K) / (f_D \sqrt{m_D} / f_\pi)$  as a function of the pion mass square  $m_\pi^2 \equiv m_{PS}(\mu_l, \mu_l, \mu_l)^2$ , in units of  $r_0$ . We display data with  $\mu_s$  and  $\mu_c$  fixed to the simulated masses that correspond to reference strange and charmed meson masses  $r_0 m_{PS}(\mu_l, \mu_s, \mu_s) = 1.63$  and  $r_0 m_{PS}(\mu_l, \mu_s, \mu_c) = 4.41$ . The SU(2)- (SU(3)-) ChPT extrapolation to the physical pion mass is represented at fixed lattice spacing by the dashed (dotted) curves, and in the continuum limit by the solid (dashed-dotted) curve. The physical results, illustrated by diamonds in the plots, are obtained from SU(2)-ChPT after interpolating to the physical strange and charm quark masses.

their deviation from the average as an additional systematic uncertainty due to the chiral extrapolation.

As in the light meson case, we estimate the uncertainty due to residual discretization effects by assigning an error of 50% to the extrapolation from our finest lattice at  $\beta = 4.05$  to the continuum limit. In the former case we obtain  $f_D^{\beta=4.05} = 208$  MeV and  $f_{D_s}^{\beta=4.05} = 257$  MeV, that are  $\simeq 5\%$  above the continuum limit estimates. Note that this effect is larger than the naïve estimate of leading discretization effects as being of  $\mathcal{O}(\alpha_s a^2 \mu_c^2)$ , which follows from the observation that  $\mathcal{O}((a\mu_c)^n)$  effects have been corrected at tree level in the definition of the decay constants. This finding clearly illustrates the importance, for lattice studies of heavy quarks, of evaluating discretization effects with simulations performed at several values of the lattice spacing, rather than on the basis of simple order of magnitude estimates. We also find that discretization effects largely cancel in the ratio of the decay constants, and we obtain  $(f_{D_s} / f_D)^{\beta=4.05} = 1.23$  from Fit II, that is only 0.8% below its continuum limit estimate. The same difference is even smaller in the case of Fit I.

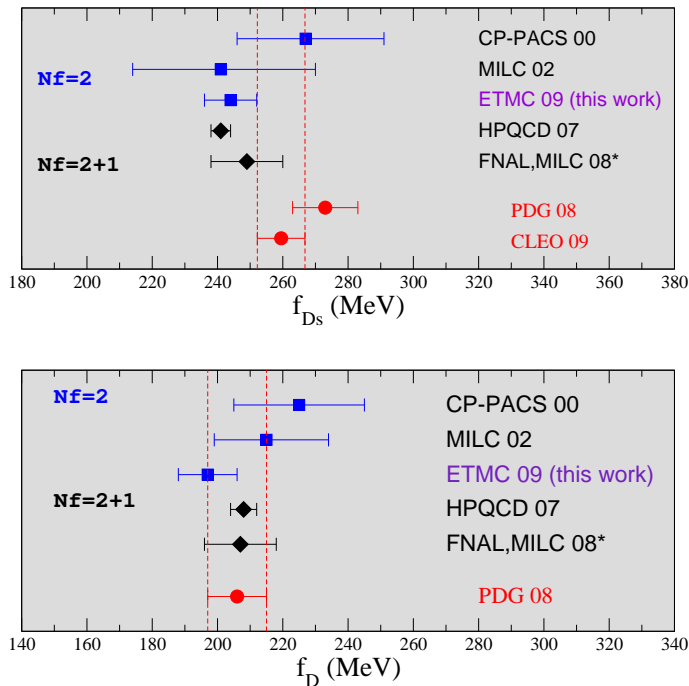


Figure 5: Lattice QCD determinations of the  $D$ -mesons decay constants  $f_{D_s}$  (top) and  $f_D$  (bottom) obtained from simulations with  $N_f = 2$  [49, 50] and  $N_f = 2 + 1$  [41, 51] dynamical fermions. A star in the legend denotes preliminary results. The lattice results for  $f_{D_s}$  are also compared with the PDG 2008 experimental average [2] and with the recent improved measurement by CLEO [3]. For  $f_D$  we compare with the CLEO determination [48].

Our final results for the  $D$  and  $D_s$  decay constants and the ratio  $f_{D_s}/f_D$  are then

$$f_D = 197(6)(2)(6) \text{ MeV} \quad , \quad f_{D_s} = 244(3)(2)(7) \text{ MeV} \quad , \quad f_{D_s}/f_D = 1.24(3)(0)(1) \quad , \quad (22)$$

where the errors come from statistics plus fitting, chiral extrapolation and discretization effects, respectively. By combining all these uncertainties in quadrature we finally obtain

$$f_D = 197(9) \text{ MeV} \quad , \quad f_{D_s} = 244(8) \text{ MeV} \quad , \quad f_{D_s}/f_D = 1.24(3) \quad . \quad (23)$$

The result obtained for  $f_D$  is in very good agreement with the CLEO measurement,  $f_D^{exp.} = 205.8(8.5)(2.5) \text{ MeV}$  [48], and with other  $N_f = 2$  [49, 50] and  $N_f = 2 + 1$  [41, 51] lattice calculations, as shown in fig. 5. Even more interesting is the comparison shown in the same figure between our result for  $f_{D_s}$ , other lattice results and the experimental measurements. The PDG 2008 average was  $f_{D_s}^{exp.} = 273(10) \text{ MeV}$  [2], higher than the values indicated by lattice calculations, for which a possible explanation as an effect of new physics was given in refs. [21, 22]. Recently, however, CLEO has performed with higher statistics an improved measurement of the branching ratio  $Br(D_s^+ \rightarrow \tau^+ \nu \rightarrow e^+ \nu \bar{\nu} \nu)$  [52] which, combined with their measurements of  $Br(D_s^+ \rightarrow \mu^+ \nu)$  and  $Br(D_s^+ \rightarrow \tau^+ \nu \rightarrow \pi^+ \bar{\nu} \nu)$ , gives  $f_{D_s} = 259.5(6.6)(3.1) \text{ MeV}$  [3]. This latter determination, being in better agreement with our and other lattice results, weakens the possibility of a new physics effect in leptonic  $D_s$  decays. In ref. [3], also an improved determination of the ratio of  $D_s$  and  $D$  decay constants is provided by CLEO,  $f_{D_s}/f_D = 1.26(6)(2)$ , which is in good agreement with our result in eq. (23).

## Acknowledgements

We thank all the members of the ETM Collaboration for fruitful discussions. D.P. thanks the Dipartimento di Fisica, Università di Roma Tre, and C.T. thanks the Laboratoire de Physique Théorique, Université de Paris XI, for the hospitality. V.L., R.F., F.M. and S.S. thank MIUR (Italy) for partial financial support under the contract PRIN06. D.P. thanks MEC (Spain) for partial financial support under grant FPA2005-00711. This work has been supported in part by the EU Contract No. MRTN-CT-2006-035482, “FLAVIANet” and by the DFG Sonderforschungsbereich/Transregio SFB/TR9-03. We also acknowledge the Consolider-Ingenio 2010 Program CPAN (CSD2007-00042).

## References

- [1] W. J. Marciano, Phys. Rev. Lett. **93** (2004) 231803 [hep-ph/0402299].
- [2] C. Amsler *et al.* [Particle Data Group], Phys. Lett. B **667** (2008) 1.
- [3] J. P. Alexander [CLEO Collaboration], arXiv:0901.1216 [hep-ex].
- [4] B. Blossier *et al.* [ETM Coll.], JHEP **0804** (2008) 020 [0709.4574 [hep-lat]].
- [5] P. Weisz, Nucl. Phys. B **212** (1983) 1.
- [6] R. Frezzotti, P. A. Grassi, S. Sint and P. Weisz [Alpha collaboration], JHEP **0108** (2001) 058 [arXiv:hep-lat/0101001].
- [7] Ph. Boucaud *et al.* [ETM Collaboration], Phys. Lett. B **650** (2007) 304 [arXiv:hep-lat/0701012].
- [8] Ph. Boucaud *et al.* [ETM collaboration], Comput. Phys. Commun. **179** (2008) 695 [arXiv:0803.0224 [hep-lat]].
- [9] C. Urbach [ETM Coll.], PoS **LAT2007** (2007) 022 [0710.1517 [hep-lat]].
- [10] P. Dimopoulos *et al.* [ETM Collaboration], arXiv:0810.2873 [hep-lat].
- [11] R. Frezzotti and G. C. Rossi, JHEP **0408** (2004) 007 [hep-lat/0306014].
- [12] A. Shindler, Phys. Rept. **461** (2008) 37 [arXiv:0707.4093 [hep-lat]].
- [13] A. X. El-Khadra, A. S. Kronfeld and P. B. Mackenzie, Phys. Rev. D **55** (1997) 3933 [arXiv:hep-lat/9604004].
- [14] C. McNeile, arXiv:0810.3791 [hep-lat].
- [15] R. Frezzotti and G. C. Rossi, JHEP **0410** (2004) 070 [arXiv:hep-lat/0407002].
- [16] A. M. Abdel-Rehim, R. Lewis, R. M. Woloshyn and J. M. S. Wu, Phys. Rev. D **74** (2006) 014507 [arXiv:hep-lat/0601036].

- [17] S. R. Sharpe and J. M. S. Wu, Phys. Rev. D **71** (2005) 074501 [arXiv:hep-lat/0411021].
- [18] R. Frezzotti, G. Martinelli, M. Papinutto and G. C. Rossi, JHEP **0604** (2006) 038 [arXiv:hep-lat/0503034].
- [19] S. R. Sharpe and Y. Zhang, Phys. Rev. D **53** (1996) 5125 [arXiv:hep-lat/9510037].
- [20] C. Allton *et al.* [RBC-UKQCD Collaboration], Phys. Rev. D **78** (2008) 114509 [arXiv:0804.0473 [hep-lat]].
- [21] B. A. Dobrescu and A. S. Kronfeld, Phys. Rev. Lett. **100** (2008) 241802 [0803.0512 [hep-ph]].
- [22] A. G. Akeroyd and F. Mahmoudi, arXiv:0902.2393 [hep-ph].
- [23] P. Dimopoulos, R. Frezzotti, G. Herdoiza, C. Urbach and U. Wenger [ETM Collaboration], PoS **LAT2007** (2007) 102 [arXiv:0710.2498 [hep-lat]].
- [24] P. Dimopoulos, R. Frezzotti, G. Herdoiza, A. Vladikas, V. Lubicz, S. Simula and M. Papinutto, PoS **LAT2007** (2007) 241 [arXiv:0710.0975 [hep-lat]].
- [25] ETM Collaboration, in preparation.
- [26] C. McNeile and C. Michael [UKQCD Coll.], Phys. Rev. D **73** (2006) 074506 [hep-lat/0603007].
- [27] L. Lellouch, arXiv:0902.4545 [hep-lat].
- [28] J. Gasser and H. Leutwyler, Annals Phys. **158** (1984) 142.
- [29] R. Sommer, Nucl. Phys. B **411** (1994) 839 [hep-lat/9310022].
- [30] J. Gasser and H. Leutwyler, Phys. Lett. B **188** (1987) 477.
- [31] D. Becirevic and G. Villadoro, Phys. Rev. D **69** (2004) 054010 [hep-lat/0311028].
- [32] S. R. Sharpe, Phys. Rev. D **56** (1997) 7052 [Erratum-ibid. D **62** (2000) 099901] [arXiv:hep-lat/9707018].
- [33] J. Noaki *et al.* [JLQCD and TWQCD Collaborations], Phys. Rev. Lett. **101** (2008) 202004 [arXiv:0806.0894 [hep-lat]].
- [34] G. Colangelo, S. Durr and C. Haefeli, Nucl. Phys. B **721** (2005) 136 [hep-lat/0503014].
- [35] R. Baron *et al.* [ETM Collaboration], PoS **LATTICE2008** (2008) 094 [arXiv:0810.3807 [hep-lat]].
- [36] K. Jansen, arXiv:0810.5634 [hep-lat].
- [37] Y. Aoki *et al.*, Phys. Rev. D **72** (2005) 114505 [hep-lat/0411006].

- [38] C. Aubin *et al.* [MILC Coll.], Phys. Rev. D **70** (2004) 114501 [hep-lat/0407028].
- [39] C. Bernard *et al.*, PoS **LAT2007** (2007) 090 [arXiv:0710.1118 [hep-lat]].
- [40] S. R. Beane *et al.*, Phys. Rev. D **75** (2007) 094501 [hep-lat/0606023].
- [41] E. Follana *et al.* [HPQCD and UKQCD Coll.], Phys. Rev. Lett. **100** (2008) 062002 [0706.1726 [hep-lat]].
- [42] S. Aoki *et al.* [PACS-CS Coll.], 0807.1661 [hep-lat].
- [43] C. Aubin, J. Laiho and R. S. Van de Water, 0810.4328 [hep-lat].
- [44] M. Antonelli *et al.* [FlaviaNet Working Group on Kaon Decays], 0801.1817 [hep-ph].
- [45] J. C. Hardy and I. S. Towner, arXiv:0812.1202 [nucl-ex].
- [46] A. Anastassov *et al.* [CLEO Collaboration], Phys. Rev. D **65** (2002) 032003 [arXiv:hep-ex/0108043].
- [47] D. Becirevic and B. Haas, arXiv:0903.2407 [hep-lat].
- [48] B. I. Eisenstein *et al.* [CLEO Collaboration], Phys. Rev. D **78** (2008) 052003 [arXiv:0806.2112 [hep-ex]].
- [49] A. Ali Khan *et al.* [CP-PACS Coll.], Phys. Rev. D **64** (2001) 054504 [hep-lat/0103020].
- [50] C. Bernard *et al.* [MILC Coll.], Phys. Rev. D **66** (2002) 094501 [hep-lat/0206016].
- [51] E. Gamiz, arXiv:0811.4146 [hep-lat].
- [52] P. U. E. Onyisi [CLEO Collaboration], arXiv:0901.1147 [hep-ex].